

Femtosecond Transient Spectroscopy and Excitonic Interactions in Photosystem I

Alexander N. Melkozernov, Su Lin, and Robert E. Blankenship*

Department of Chemistry and Biochemistry, Center for the Study of Early Events in Photosynthesis, Arizona State University, Tempe, Arizona 85287-1604

Received: September 14, 1999; In Final Form: November 11, 1999

Ultrafast dynamics of excitation transfer in the Photosystem I (PSI) core antenna from the cyanobacterium *Synechocystis* sp. PCC 6803 were detected at 77 K by using femtosecond transient absorption spectroscopy with selective excitation at 700, 695, and 710 nm. At low temperature, the efficiency of uphill energy transfer in the core antenna significantly decreases. As a result, the spectral profile of the PSI equilibrated antenna shifts to lower energies because of a change of chlorophyll (Chl) excited-state distribution. Observed on a 2-ns time scale, P_{700} photooxidation spectra are largely excitation wavelength independent. In the early time spectra, excitation of P_{700} induces transient photobleaching at 698 nm accompanied by a resonant photobleaching band at 683 nm decaying within 250–300 fs. Chemical oxidation of P_{700} does not affect the transient band at 683 nm. This band is also present in 200-fs spectra induced by selective excitation of Chls at 710 nm (red pigments C708), which suggests that this high-energy transition may reflect an excitonic interaction between pigments of the reaction center and closely located red pigments. Possible candidates for the interacting molecules in the 4-Å crystal structure of cyanobacterial PSI are discussed.

Introduction

The Photosystem I (PSI) core antenna of oxygenic photosynthetic organisms functions as an effective converter of solar energy captured by a network of chlorophyll *a* (Chl *a*) molecules of the core antenna into the energy of primary charge separation mediated by redox-active Chl *a* molecules of the PSI reaction center (RC). The primary energy conversion steps take place within two transmembrane protein subunits, PsaA and PsaB. However, an assembly of 11 protein subunits is required for the light-driven transmembrane electron transfer from plastocyanin (or cytochrome *c*) to ferredoxin.¹ A 4-Å structural model of the PSI from the cyanobacterium *Synechococcus elongatus*^{2,3} identified 83 Chl *a* molecules of the core antenna and 6 Chl *a* molecules, 2 phylloquinones, and 1 Fe–S cluster of the RC bound to the PsaA–PsaB heterodimer.

All chlorophyll *a* molecules of the PSI core contribute to the Q_y absorption band in the 640–720-nm region. Although the majority of the pigments dominate the steady-state absorption of the cyanobacterial PSI core, the low-energy wing of the absorption band has contributions from pigments of the RC as well as low-energy antenna Chls or red pigments absorbing in the 700–720-nm region.^{1,4,5} The major problem in identifying of the spectral forms is their overlap and inhomogeneous broadening. The ratio of excitonic coupling between pigments to the spectral disorder in the PSI is less than unity,^{6–8} which implies that the excitation dynamics is in a hopping limit resulting from a Förster inductive resonance mechanism. Fast broadening processes in PSI mask possible transients resulting from excitonic interactions in the RC and antenna. At room temperature, pigment excitation in the PSI core equilibrates relatively fast among all spectral forms including the red

pigments within 2–10 ps.^{9–18} Recently, subpicosecond uphill and downhill energy-transfer processes were resolved in cyanobacterial PSI^{16,19–21} and P_{700} -enriched PSI from higher plants.^{22,23}

At low temperatures, slowing of energy-transfer rates and localization of excitations in PSI were reported.^{4,24} To what extent the excitation equilibrates is an open question. Even at very low temperatures, a high quantum yield for charge separation is still observed upon excitation of the core pigments including red pigments.^{5,7,25,26} Reversible photochemistry is observed at 77 K in 45% of the PSI from the cyanobacterium *S. elongatus*.²⁷

The structure of the photosystem I RC reveals a dimer of two chlorophylls located on the lumenal side of the membrane with a center-to-center distance of 6.9 Å (interplane distance of ~4.0 Å). This dimer is ascribed to the primary electron donor P_{700} , which is equidistant (20–30 Å) from the surrounding core antenna. Close to P_{700} , four monomeric Chl *a* are arranged in two pairs symmetrically located along the pseudo- C_2 axis running through P_{700} and the iron–sulfur cluster F_X . The interpigment distances among the RC Chls would allow an excitonic coupling in the dimer of P_{700} and between the primary donor and Chl *a* monomers of the RC.²⁸ An upper excitonic component of P_{700} was predicted at 695,²⁹ 650,³⁰ and 682 nm.¹ Recent Raman scattering study of the PSI core from *Synechocystis* sp. PCC 6803³¹ indicates a strong coupling of monomeric Chls of the RC with P_{700} and ultrafast relaxation of P_{700} *. The presence of 3–4 Chls absorbing around 695 nm that are closely associated with P_{700} was suggested on the basis of thermodynamic analysis of the absorption and fluorescence spectra of PSI-200 particles from higher plants.³²

Frequency domain studies of the red wing of the PSI absorption band revealed a stronger electron–phonon coupling in the region of P_{700} in PSI-200 particles from higher plants^{33,34} and in the region of red pigment absorption at 708 nm in the PSI from *Synechocystis* sp.^{5,25} Strong electron–phonon coupling

* To whom correspondence should be addressed. Mailing address: Department of Chemistry and Biochemistry, Arizona State University, Tempe, AZ 85287-1604. Phone: 480-965-1439. Fax: 480-965-2747. E-mail: Blankenship@asu.edu.

indicates increased pigment–pigment interactions consistent with the dimer nature of P_{700} and suggestions of Chl dimer formation for red pigments in cyanobacteria.⁵

The current PSI structure (Protein Data Base accession number 2PPS) shows that in the core antenna surrounding the RC, 24 of the 83 identified Chls have center-to-center distances shorter than 10 Å. Four of these “tightly packed” pigments that form two dimers in close proximity to A_0 (the primary acceptor) in one of the two symmetry-related sites in the RC of PSI were suggested to be the likely candidates for red pigments in the cyanobacterial Photosystem I.²⁰ Selective excitation of the red pigments at 710 nm induces the 380-fs uphill energy transfer from red pigments to Chl *a* species absorbing around 696–700 nm, which suggests a close location of the long-wavelength absorbing Chls to the RC.²⁰ Larson and Owens³⁵ concluded that the majority of red pigments must be among the group of chlorophylls closest to P_{700} , including electron-transfer components, connecting chlorophylls, and some pigments of the surrounding bulk antenna. A recent fluorescence study of subunit-deficient mutant PSI from *Synechocystis* *sp.* reported that red pigments are bound to PsaA–PsaB subunits.³⁶ However, reports of Gobets et al.^{16,37} based on time-resolved fluorescence and modeling claim that the red pigments in *Synechocystis* *sp.* are not in contact with the RC.

In attempts to probe excitonic interactions of the pigments in the Photosystem I core and RC, we performed a 77 K ultrafast transient absorption study of the PSI from cyanobacterium *Synechocystis* *sp.* PCC 6803 under multicolor excitation with 150-fs spectrally narrowed (fwhm = 5 nm) pulses. When the temperature is lowered, the uphill energy transfer in the PSI core significantly decreases, and new spectral features in the neighborhood of P_{700} are revealed. Excitation at 695, 700, and 710 nm shows that the Chl molecules absorbing in this spectral region, including red pigments, are either coupled or relatively closely located with respect to each other, thus giving rise to subpicosecond dynamics at 683 nm.

Materials and Methods

Isolation of Photosystem I Particles. PSI particles were isolated from the PS II-less mutant psbDI/C/DII of cyanobacterium *Synechocystis* *sp.* PCC 6803 as described earlier.¹¹ The Chl *a*/ P_{700} ratio in a mixture of PS I monomers and trimers was about 90.

Transient Absorption Spectroscopy. For time-resolved absorption spectroscopy at 77 K, the sample was resuspended in 20 mM Tris HCl buffer, pH 8.0, 100 mM $MgCl_2$, 0.03% β -dodecyl maltoside, 20 mM sodium ascorbate, and 15 μ M phenazine methosulfate (PMS). The mixture contained 67% glycerol (v/v). A 200- μ L sample was placed in an optical cell between two plexiglass windows with an optical path of 1.2 mm. The Chl *a* concentration in the sample in all experiments was about 80 μ g/mL. The optical cell was put in a closed-cycle helium cryostat (APD Cryogenics) and slowly cooled to 77 K without sample cracking.

The transient absorption spectra of the photosystem I core antenna at 77 K were measured by using a femtosecond laser spectrometer operating at 1 kHz as described earlier.^{20,38} Transient absorption spectra were measured at the magic angle on 2- and 10-ps time scales in the 600–750-nm spectral region. Samples were excited at 670, 680, 695, 700, and 710 nm by using laser pulses with spectral width of 5 nm (fwhm) and pulse duration of 150 fs (fwhm). The intensity of the pump pulses was kept low enough to avoid singlet–singlet annihilation (less than 1 photon per RC). Long-lived spectral changes resulting

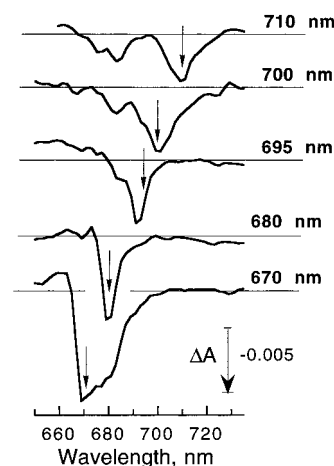


Figure 1. Excitation wavelength dependence of initial transient spectra of the Photosystem I core from *Synechocystis* *sp.* PCC 6803 recorded at 77 K. Excitations are at 710 (pump–probe delay of 204 fs), 700 (290 fs), 695 (195 fs), 680 (272 fs), and 670 nm (270 fs).

from possible accumulation of P_{700}^+ in the sample due to irreversible photochemistry at low temperatures ($\sim 55\%$ at 77 K²⁷) were subtracted from the transient spectra as a background.

The global analysis and decay-associated spectra (DAS) were constructed after deconvolution of the observed kinetics with the excitation pulse and correction for the spectral dispersion of the pump beam as described earlier.²⁰

Molecular graphics in Figure 7 was performed by using WebLab ViewerLite 3.10 (Molecular Simulations) and PDB coordinates of PSI (accession number 2PPS).

Results

Dynamic Hole-Burning of the Chl *a* Q_y Transition Band in the PSI Core at 77 K. Figure 1 compares the initial transient spectra obtained with excitation at different characteristic wavelengths over the Chl *a* Q_y transition band of the PSI core antenna at 77 K. The width of the excitation pulse was 5 nm (~ 100 cm^{-1}) at all excitation wavelengths. The initial spectral changes observed within the first 200 fs are strongly excitation wavelength dependent and reflect the dynamic spectral hole-burning of the Chl *a* Q_y transition band in the PSI core. Excitation into the blue edge of the absorption band at 670 nm results in an initial photobleaching band centered at 670 nm, broadened by a shoulder around 680 nm. However, a shift of the excitation wavelength close to the maximum of the absorption band at 680 nm produces a very narrow photobleaching band with a spectral width (fwhm = 120 cm^{-1}) that largely follows the width of the excitation pulse.

Excitation into the red edge of the PSI absorption band where the pigments of the RC absorb produces a substantially different spectral profile at early times. The initial spectrum with excitation at 695 nm is broader (fwhm = 150 cm^{-1}) than the spectrum with 680-nm excitation and is blue shifted with a center at 691 nm. The band is asymmetric with a weak shoulder around 685 nm. This shoulder is resolved as a separate band peaked at 683 nm resonant with the photobleaching band upon excitation of P_{700} at 700 nm. The width of the major photobleaching band at 700 nm is 330 cm^{-1} . This two-band structure is preserved in a 204-fs transient absorption spectrum induced by selective excitation into the region of red pigment's absorption at 710 nm. The photobleaching band at 710 nm (fwhm = 240 cm^{-1}) is accompanied by a resonant photobleaching band at 683 nm and a partially resolved band at 675 nm. The ratio

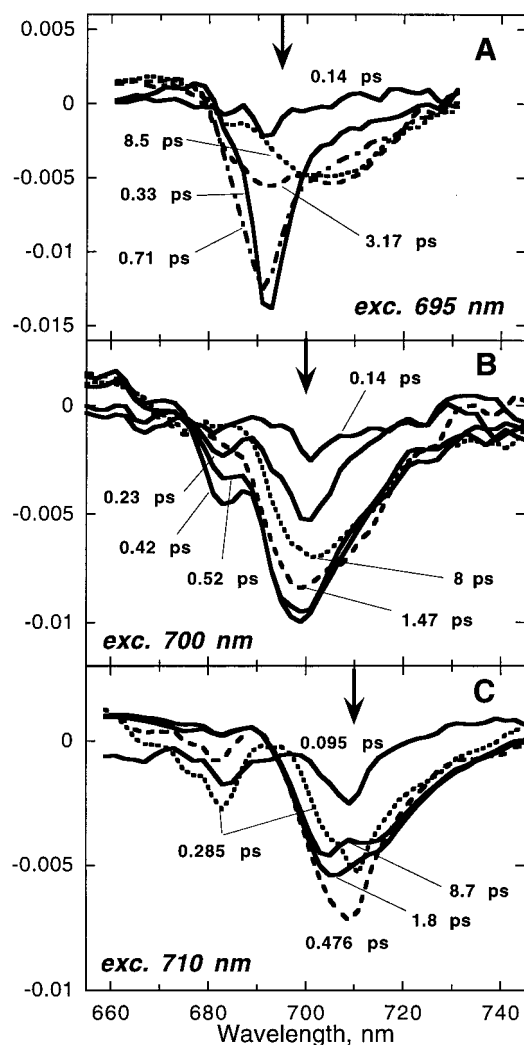


Figure 2. Transient absorption spectra of the Photosystem I core from *Synechocystis* sp. PCC 6803 measured at 77 K on a 10-ps time scale with excitation at 695 (A), 700 (B), and 710 nm (C) and different representative pump-probe delays.

of ΔA_{683} and ΔA at the pump wavelength is higher with the 710-nm excitation.

Dynamics of the Transient Absorption within 10 ps. Spectral evolution of the observed two-band structure within the first 10 ps upon excitation at 695, 700, and 710 nm is shown in Figure 2. The decay associated spectra (DAS) obtained after global analysis of data are presented in Figure 3.

The initial transient changes obtained with excitation at 695 nm at 77 K are unusually narrow (fwhm ~ 100 cm^{-1}) (Figure 2A). Similar changes were observed at room temperature.²⁰ The center of transient photobleaching is at 691 nm. The rate of broadening of the band is much slower compared with the rate of initial spectral broadening with excitation at 700 or 710 nm (Figure 2B and C). The structure at 683 nm is pronounced as a weak shoulder or a slight asymmetry in the spectra within the first 400 fs while the band reaches a maximum (Figure 2A). The population of excited Chls at 691 nm decays very fast with two exponential components of 200 fs and 4.6 ps (Figure 3A). The latter component reflects an energy transfer that populates a broad band of Chl *a* spectral forms absorbing at 700–710 nm. Within 10 ps, the photobleaching maximum shifts from 691 to 705 nm (see spectra at 0.71 and 8.5 ps in Figure 2A and 4.6 ps DAS in Figure 3A). The nondecaying component (Figure 3A) is similar to that obtained with 700-nm excitation; however,

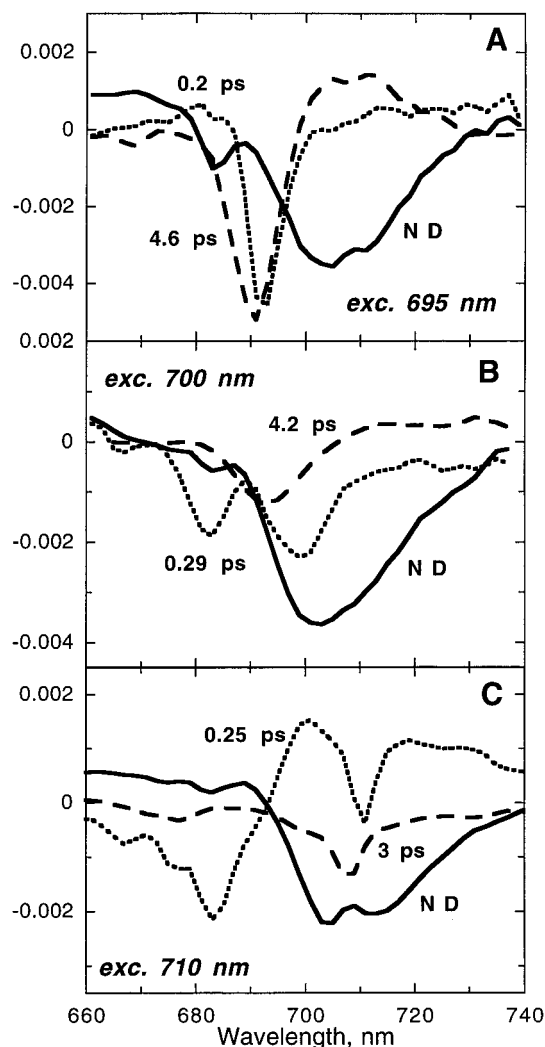


Figure 3. Decay associated spectra obtained after global analysis of transient kinetics on the 10-ps time scale with excitation at 695 (A), 700 (B), and 710 nm (C).

the photobleaching at 683 nm is more pronounced, and a shoulder is apparent at 712 nm.

Selective excitation of P_{700} induces a broad initial photobleaching at 700 nm. This photobleaching is resonant with a ΔA band at 683 nm (Figure 2B). Progressive decrease of the ratio $\Delta A_{683}/\Delta A_{700}$ indicates both a decay of ΔA_{683} and a further increase of photobleaching at 700 nm. The transient band at 683 nm decays within 290 fs (Figure 3B). A subpicosecond decay component of the ΔA_{700} band has a similar lifetime (see 290-fs DAS in Figure 3B).

The ΔA_{700} band reaches a maximum at 0.52-ps pump-probe delay, and its peak shifts to 698 nm. The early time broadening (from 330 cm^{-1} in the 140-fs spectrum to 470 cm^{-1} in the 520-fs spectrum) most likely contains a contribution from the buildup of stimulated emission. However, the further broadening (up to 520 cm^{-1} in the 8-ps spectrum) that accompanies the decay of the band is followed by a red spectral shift from 698 to 703 nm. This shift is a manifestation of an excitation equilibration phase featuring both decay around 693 nm and appearance of a broad ΔA band in the region where red pigments absorb, with a lifetime of 4–6 ps (4.2-ps DAS in Figure 3B). Relaxation of this broad band is followed by trapping that is not resolved on this time scale, which is presented in Figure 3B as a nondecaying component characterized by a broad asymmetric band centered at 703 nm and a small band at 683 nm that appears again after

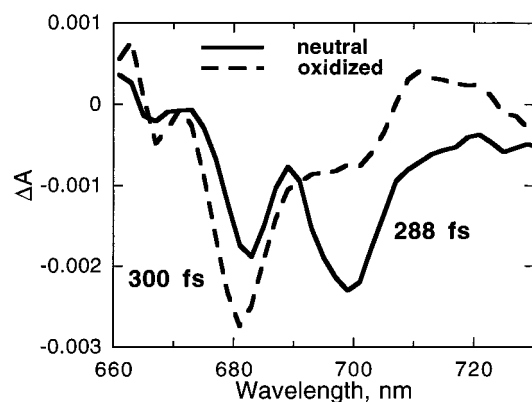


Figure 4. Comparison of decay associated spectra of the shortest kinetic components obtained with excitation at 700 nm from neutral Photosystem I (solid line) and oxidized Photosystem I (dashed line). P_{700} was chemically oxidized in a sample with 3 mM potassium ferricyanide and continuous white-light illumination for 20 min upon cooling the sample to 77 K. Spectra are not normalized. Data taken on 10-ps time scale.

nearly complete decay at an earlier time. This DAS represents a mixture of longer-living trapping on both P_{700} and the red pigments absorbing at 708 nm and the P_{700} photooxidation.

Selective excitation of the red pigments at 710 nm induces a resonant photobleaching at 683 nm (Figures 1 and 2C). The ΔA_{683} band decays within 250 fs, whereas the band at 710 nm reaches a maximum within 500 fs (Figure 2C). During the first picosecond, the exciton relaxation of the band results in a symmetric broadening from 140 to 450 cm^{-1} . A 250-fs DAS represents a subpicosecond dynamics that includes decay of excited states at 710 and 683 nm accompanied by a buildup of positive ΔA around 690–700 nm and below 710 nm, which is a mixture of newly appeared transient bands, stimulated emission, and Chl excited-state absorption (Figure 3C). Within 10 ps, the redistribution of the excitation results in the appearance of two ΔA bands at 705 and 715 nm. These bands are nondecaying on that time scale. The nondecaying exponential component (Figure 3C) reflects a longer-lived trapping of the excitation by P_{700} followed by P_{700} photooxidation as well as trapping on the red pigments.

To probe whether the transition at 683 nm in the initial transient spectra belongs to P_{700} , we compared the spectra of the subpicosecond decay in neutral and oxidized PSI with excitation at 700 nm (Figure 4). In the PSI sample with oxidized P_{700} the 300-fs DAS is dominated by a spectral band at 683 nm, in contrast to the two-band structure in the subpicosecond DAS of neutral PSI.

P_{700} Photooxidation Spectra at 77 K. At low temperatures, a reasonably high quantum yield for charge separation in the RC of cyanobacterial PSI is observed.^{5,7,25,26} Data of Schlodder et al.²⁷ show that about 45% of the PSI from cyanobacterium *S. elongatus* perform reversible photochemistry at 77 K. On the 200-ps and 2-ns time scales, excitation trapping by P_{700} and red pigments at 77 K can be resolved (data not shown). The absorption changes of P_{700} upon photooxidation obtained with pump–probe delays of 1.5–2 ns and excitation at 695, 710, and 720 nm at 77 K are shown in Figure 5. The spectra are similar in shape to P_{700} photooxidation spectra of PSI from *Synechocystis* sp. at room temperature²⁰ and largely follow the shape of P_{700} photooxidation spectra of the PSI core from cyanobacterium *S. elongatus* recorded at 5 K.²⁶ Spectral changes due to long-lived excited states of red pigments also might contribute to the spectra in Figure 5.

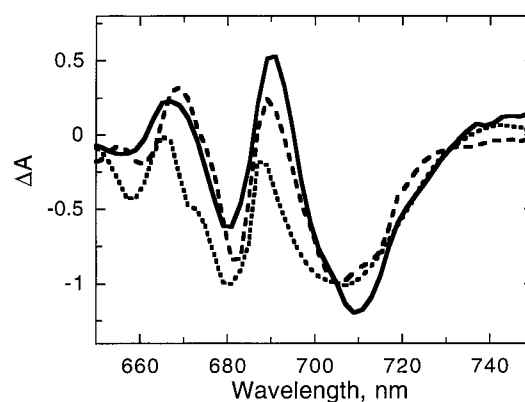


Figure 5. 77 K absorption difference spectra of photosystem I core obtained at time delays of ~ 2 ns with excitations at 695 (dotted line), 710 (solid line), and 720 nm (dashed line). Spectra were normalized at 705 nm.

Discussion

For the PSI core antenna, the ratio of excitonic coupling and the spectral disorder (both homogeneous and inhomogeneous) is believed to be much less than unity, which suggests that the interaction between Chls is weak and within the incoherent hopping limit.^{6,7} However, the two processes, excitation hopping and exciton relaxation, clearly coexist in the photosynthetic antenna.^{6,8} The present paper addresses the issue of excitonic interactions in the PSI core from cyanobacterium *Synechocystis* sp. PCC 6803 on the basis of femtosecond absorption spectroscopy at 77 K.

Dynamic hole-burning of the Q_y transition illustrates a significant inhomogeneity of the Chl *a* spectral forms (Figure 1). A narrow initial spectrum excited at 680 nm most likely reflects a strong exciton transition of bulk Chl *a*. Although the Gaussian distribution of center-to-center distances in the PSI core has two peaks at 11 and 14.8 Å,³⁹ 24 of the 83 Chl *a* molecules have intercenter distances closer than 10 Å, indicating stronger interactions of pigments. The width of the initial spectrum induced at 670 nm is strikingly broader. A global analysis of the transient spectra within 2 ps reveals a subpicosecond energy-transfer process with a spectral shift from 670 to 680 nm (data not shown).

A common feature of the spectral changes induced by excitations at 695, 700, and 710 nm is a red shift of the spectral profiles of overall decay. This is a clear indication of significantly reduced uphill energy-transfer processes at 77 K (Figure 2). Recently, we showed that at room temperature, excitation of the PSI from *Synechocystis* sp. PCC 6803 within a major Q_y transition of Chl *a* induces progressive broadening of initial transient absorption spectra within 2–3 ps in both red and blue directions indicative of downhill and uphill energy transfer, respectively.²⁰ Upon excitation at 710 nm, a broad shoulder extending from 700 to 680 nm on the high-energy side of the initial transient spectra and the shape of the 380-fs DAS were interpreted as reflecting a subpicosecond uphill energy transfer from red pigments absorbing at 708 nm to Chl *a* spectral forms absorbing in the 690–700 nm region (see Figures 2E and 3C in ref 20). The absence of the blue-shifted broadening at 77 K made revealing new spectral features around 683 nm possible in the early time spectra upon selective excitation into the red wing of the PSI absorption band. The absorption changes in the early time spectra not broadened by relaxation processes revealed in the present work are a manifestation of excitonic interactions among the Chls of PSI that probably have some

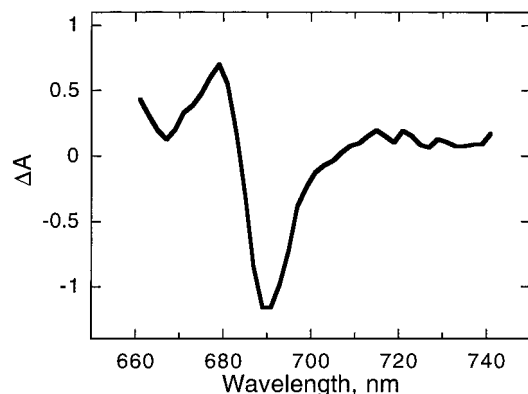


Figure 6. Difference spectrum $A_0 - (A_0^- + A_0^*)$ obtained as a difference of the 3.17-ps spectrum in Figure 2B and the P_{700} photo-oxidation spectrum (averaged spectra in Figure 5). Before subtraction spectra were normalized at 705 nm.

contributions into spectral broadenings of initial ΔA at room temperature.²⁰

One of the possible explanations of a simultaneous photobleaching within 200 fs in ΔA bands at 700 and 683 nm upon selective excitation of P_{700} (Figures 1 and 2) is that the transient band at 683 nm represents an upper excitonic component of P_{700} . This would agree with the prediction of Brettel,¹ who concluded that the upper excitonic component is 18 nm shifted relative to the lower excitonic component (370 cm^{-1}), and estimations of Beddard²⁸ based on the crystal structure of PSI. However, oxidation of P_{700} does not eliminate the transient band at 683 nm (Figure 4), which suggests that this transition probably does not belong to the P_{700} dimer and is not an optical transition of monomers in the dimer.

The transient changes at 683 nm may reflect excitonic transitions of Chls located very close to P_{700} such as accessory Chls eC2 (eC2') located between P_{700} and A_0 (eC3 (eC3')) or even the A_0 molecule itself in either branch of potential electron-transfer cofactors in the RC.^{2,3} To test this possibility, we selectively excited Chls absorbing at 695 nm. At room temperature in the cyanobacterial PSI, absorption changes in the 687–695 nm spectral region upon chemical reduction of secondary acceptors in the RC were ascribed to photoreduction of the primary acceptor A_0 .^{1,40,41} If the transient ΔA_{683} is coupled with the A_0 photoreduction band, then selective excitation at 695 nm might induce the resonant band at 683 nm. A shoulder at 685 nm in the 200-fs spectrum (Figure 1) may suggest the coupling of transition excited at 695 nm with the 683-nm band. However, experimental noise and a limit of time resolution make these data less conclusive.

The 3.17-ps spectrum (Figure 2A) may represent a mixture of excited A_0^* (or A_0^-), P_{700}^+ , and excited red pigments. Subtraction of the 77 K P_{700} photooxidation spectrum (average of spectra in Figure 5) from the 3.17-ps spectrum in Figure 3A gives a narrow spectrum centered at 690 nm (Figure 6) that is strikingly close in shape to the A_0^- photoreduction spectra reported earlier for cyanobacteria and higher plants at room temperature.^{40,41} The initial spectra with 695-nm excitation might therefore reflect a mixture of A_0^- and A_0^* that makes the redox-active A_0 and its symmetric counterpart indistinguishable. However, the fact that the 683-nm band is poorly resolved in the initial spectra with 695-nm excitation may also suggest that the 691-nm transition in Figure 2A is dominated within several hundred femtoseconds by excitation of a transition weakly coupled with the 683-nm transition.

The structural model of the PSI is available only for *S. elongatus*.^{2,3} However, the wavelength positions of Chl *a*

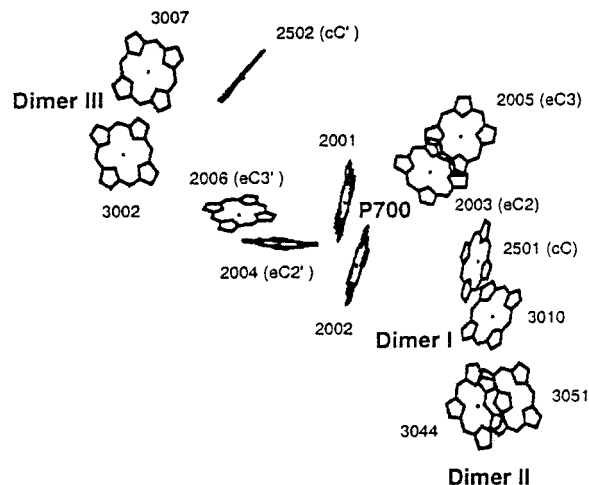


Figure 7. Local structure of the pigments in the RC and the nearest core antenna. P_{700} , a dimer of Chls 2001 and 2002; eC2, accessory Chl 2003; eC2', symmetric accessory Chl 2004; eC3, Chl 2005, a potential primary acceptor A_0 ; cC, connecting Chl 2501; cC', symmetric connecting Chl 2502; dimers I, II and III, antenna Chls. Atom coordinates of the Chl *a* molecules and their identification numbers in the PSI structure are taken from Protein Data Base (accession number 2PPS).² See text for details of interpigment distances. The majority of the surrounding antenna Chls were removed for clarity.

spectral forms in low-temperature absorption spectra of PSI from *Synechocystis* and *Synechococcus* are largely similar except for the presence of a second pool of red pigments at 719 nm in the PSI from *Synechococcus*.^{5,25} The fact that oscillator strengths of the bands are not identical may indicate real structural differences between the two complexes. However, these differences may be insignificant. In the strong exciton coupling limit, seemingly insignificant changes in pigment orientation or configuration may cause significant changes in absorption spectra. A very well known example is the nearly identical crystal structures of the FMO proteins from *Prosthecochloris aestuarii* and *Chlorobium tepidum*, with significant spectral differences.⁴²

We think that the local asymmetry around eC3 and eC3' Chls of the RC may shed light on the origin of the observed subpicosecond changes (Figures 1 and 2). Recently, we suggested that two separate dimers of antenna Chls located in the vicinity of one of the eC3 molecules may function as red pigments.²⁰ Dimer I (Figure 7) consists of a connecting Chl cC and an antenna Chl that is only 6.4 Å apart from the linker (interplane distance as close as 4.3 Å). Dimer II contains two totally overlapped Chls (interplane distance of 5 Å). The interplane distance between the adjacent Chls of the two dimers is 9.2 Å, and that between the linker and eC3 is 7 Å. The structure in Figure 7 shows that the eC3 Chl of the RC and the dimers are close enough to be excitonically coupled. This possibility is supported also by recent conclusions about the excitonic coupling of pigments in the PSI RC.^{31, 35}

The resonant subpicosecond photobleaching at 683 nm that accompanies excitation of red pigments (Figures 1 and 2C) and a higher ratio of ΔA_{683} and ΔA at the pump wavelength with the 710-nm excitation indicates a direct coupling of red pigments with the 683-nm transition. For excitonically coupled Chls, the distribution of a dipole strength between exciton states is determined by the orientation of the molecules. On the basis of the current crystal structure, we suggest that the transient 683-nm band is an upper excitonic component of one of the dimers that we ascribed to red pigments, most likely dimer II (Figure

7). In the case of totally overlapped monomers in dimer II, the lower excitonic transition would be suppressed, thereby giving rise to only an upper excitonic component. Estimation of coupling in the dimer II on the basis of assumption of parallel Q_y dipoles gives $\sim 680 \text{ cm}^{-1}$, which is larger than the energy difference between the 683-nm transition and the 708-nm transition (520 cm^{-1}). The excitonic interaction in dimer I closest to the eC3 molecule may contribute to the lower excitonic band at 708 nm in the PSI from *Synechocystis* sp. The absorption band at 708 nm is heterogeneously broadened at low temperatures⁵ and may have contributions of excitonic transitions of the Chls of the core antenna. For example, dimer III, located in the surrounding antenna (Figure 7), has a center-to-center distance of 8.8 Å between monomers and represents an alternative geometry of the interacting pigments translated relative to each other. Such a geometry may result in suppression of the upper excitonic component and dominance of the lower energy transitions. Knowledge of the orientation of Q_y transitions in the interacting Chls is needed to resolve a composite character of the band.

The absence of a resonant transient band at 700 nm in the initial spectra with excitation at 710 nm (Figure 2C) suggests that the P_{700} transition does not have a coherent interaction with the red pigment's transition, which is expected from the structure in Figure 7. However, comparison of transient spectra at 285 fs and 2 ps (Figure 2C) clearly shows that within this time P_{700} becomes excited because of the good spectral overlap of red pigment absorption and the P_{700} band. This is in agreement with results of our room-temperature experiments suggesting a relatively close location of the long wavelength absorbing Chls to the RC.²⁰

The 8.7-ps spectrum in Figure 2C shows that excitation at 710 nm also populates longer wavelength absorbing pigments. The nondecaying spectrum in Figure 3C and transient kinetics at 719 nm (not shown) clearly show formation of a long-lived pool of red pigments that decays within hundreds of picoseconds and on the nanosecond time scale (data not shown). Steady-state absorption spectroscopy and site-selection fluorescence spectroscopy of the PSI from *Synechocystis* sp.⁵ did not show the presence of a second pool of red pigments at 715–720 nm, in contrast to PSI from *S. elongatus*, which contains red Chls absorbing at 716 nm.²⁵ However, our finding is in agreement with the recent observation of a second pool of red pigments in PSI from *Synechocystis* at room temperature.²¹

In conclusion, selective excitation of Chl *a* spectral forms absorbing on the red edge of the Q_y transition band at 77 K in the PSI core induces at least three kinetic processes in the core antenna and the RC: (1) subpicosecond exciton dynamics featuring the appearance of a transient band at 683 nm that is resonant with a transition excited either at 700 or 710 nm; (2) spectral broadening of the major photobleaching bands resulting from exciton relaxation or excitation equilibration via downhill energy transfer; (3) long-lived trapping of the excitation by P_{700} and a pool of red pigments followed by P_{700} photooxidation. Excitation at 695, 700, and 710 nm shows that the Chl molecules absorbing in this spectral region are either coupled or located relatively close to each other.

Acknowledgment. The work was supported by National Science Foundation Grant MCB-9727607 to R.E.B. This is publication no. 421 of the Center for the Study of Early Events in Photosynthesis at Arizona State University.

References and Notes

- Brettel, K. *Biochim. Biophys. Acta* **1997**, *318*, 322.
- Schubert, W.-D.; Klukas, O.; Krauss, N.; Saenger, W.; Fromme, P.; Witt, H. T. *J. Mol. Biol.* **1997**, *272*, 741.
- Krauss, N.; Schubert, W.-D.; Klukas, O.; Fromme, P.; Witt, H. T.; Saenger, W. *Nature Struct. Biol.* **1996**, *3*, 965.
- Van Grondelle, R.; Dekker, J. P.; Gillbro, T.; Sundström, V. *Biochim. Biophys. Acta* **1994**, *1187*, 1.
- Gobets, B.; van Amerongen, H.; Monshouwer, R.; Kruij, J.; Rögner, M.; van Grondelle, R.; Dekker, J. P. *Biochim. Biophys. Acta* **1994**, *1188*, 75.
- Sundström, V.; Pullerits, T.; van Grondelle, R. *J. Phys. Chem. B* **1999**, *103*, 2327.
- Fleming, G. R.; Van Grondelle, R. *Curr. Opin. Struct. Biol.* **1997**, *7*, 738.
- Laible, P. D.; Knox, R. S.; Owens, T. G. *J. Phys. Chem. B* **1998**, *102*, 1641.
- Klug, D. R.; Giorgi, L.; Crystal, B.; Barber, J.; Porter, G. *Photosynth. Res.* **1989**, *22*, 277.
- Du, M.; Xie, X.; Jia, Y.; Mets, L.; Fleming, G. R. *Chem. Phys. Lett.* **1993**, *201*, 535.
- Hastings, G.; Kleinherenbrink, A. M.; Lin, S.; Blankenship, R. E. *Biochemistry* **1994**, *33*, 3185.
- Hastings, G.; Hoshina, S.; Webber, A. N.; Blankenship, R. E. *Biochemistry* **1995**, *34*, 15512.
- White, N. T. H.; Beddard, G. S.; Thorne, J. R. G.; Feehan, T. M.; Keyes, T. E.; Heathcote, P. J. *J. Phys. Chem.* **1996**, *100*, 12086.
- Turconi, S.; Schweitzer, G.; Holzwarth, A. R. *Photochem. Photobiol.* **1993**, *57*, 113.
- Turconi, S.; Kruij, J.; Schweitzer, G.; Rögner, M.; Holzwarth, A. R. *Photosynth. Res.* **1996**, *49*, 263.
- Gobets, B.; van Stokkum, I. H. M.; van Mourik, F.; Rögner, M.; Kruij, J.; Dekker, J. P.; van Grondelle, R. In *Photosynthesis: Mechanisms and Effects*; Garab, G., Ed.; Kluwer Academic Publishers: Dordrecht, **1998**; pp 571–574.
- Holzwarth, A. R.; Schatz, G.; Brock, H.; Bittersman, E. *Biophys. J.* **1993**, *64*, 1813.
- Byrdin, M.; Rimke, I.; Flemming, C.; Schlodder, E.; Roelofs, T. A. In *Photosynthesis: Mechanisms and Effects*; Garab, G., Ed.; Kluwer Academic Publishers: Dordrecht, **1998**; pp 567–570.
- Melkozernov, A. N.; Lin, S.; Blankenship, R. E. In *Photosynthesis: Mechanisms and Effects*; Garab, G., Ed.; Kluwer Academic Publishers: Dordrecht, **1998**; pp 405–408.
- Melkozernov, A. N.; Lin, S.; Blankenship, R. E. *Biochemistry* **2000**, in press.
- Savikhin, S.; Xu, W.; Soukoulis, V.; Chitnis, P. R.; Struve, W. *Biophys. J.* **1999**, *76*, 3278.
- Kumazaki, S.; Ikegami, I.; Yoshihara, K. *J. Phys. Chem. A* **1997**, *101*, 597.
- Kumazaki, S.; Furusawa, H.; Yoshihara, K.; Ikegami, I. In *Photosynthesis: Mechanisms and Effects*; Garab, G., Ed.; Kluwer Academic Publishers: Dordrecht, **1998**; pp 575–578.
- Lyle, P. A.; Struve, W. S. *Photochem. Photobiol.* **1991**, *53*, 359.
- Pålsson, L.-O.; Dekker, J. P.; Schlodder, E.; Monshouwer, R.; van Grondelle, R. *Photosynth. Res.* **1996**, *48*, 239.
- Pålsson, L.-O.; Flemming, C.; Gobets, B.; van Grondelle, R.; Dekker, J. P.; Schlodder, E. *Biophys. J.* **1998**, *74*, 2611.
- Schlodder, E.; Falkenberg, K.; Gergeleit, M.; Brettel, K. *Biochemistry* **1998**, *37*, 9466.
- Beddard, G. S. *J. Phys. Chem. B* **1998**, *102*, 10966.
- Schaffernicht, H.; Junge, W. *Photochem. Photobiol.* **1981**, *34*, 223.
- Vrieze, J. P.; Gast, P.; Hoff, A. J. In *Research in Photosynthesis*; Murata, N., Ed.; Kluwer Academic Publishers: Dordrecht, **1992**; pp 553–556.
- Stewart, D. H.; Cua, A.; Bocian, D. F.; Brudvig, G. W. *J. Phys. Chem. B* **1999**, *103*, 3758.
- Croce, R.; Zucchelli, G.; Garlaschi, F. M.; Bassi, R.; Jennings, R. C. *Biochemistry* **1996**, *35*, 8572.
- Gillie, J. K.; Fearey, B. L.; Hayes, J. M.; Small, G. J.; Golbeck, J. H. *Chem. Phys. Lett.* **1987**, *134*, 316.
- Gillie, J. K.; Lyle, P. A.; Small, G. J.; Golbeck, J. H. *Photosynth. Res.* **1989**, *22*, 233.
- Larson, D. R.; Owens, T. G. *Biophys. J.* **1999**, *76*, A248.
- Soukoulis, V.; Savikhin, S.; Xu, W.; Chitnis, P. R.; Struve, W. *Biophys. J.* **1999**, *76*, 2711.
- Gobets, B.; Dekker, J. P.; van Grondelle, R. In *Photosynthesis: Mechanisms and Effects*; Garab, G., Ed.; Kluwer Academic Publishers: Dordrecht, **1998**; pp 503–508.
- Freiberg, A.; Timpmann, K.; Lin, S.; Woodbury, N. W. *J. Phys. Chem.* **1998**, *102*, 10974.
- Beddard, G. S. *Philos. Trans. R. Soc. London* **1998**, *356*, 421.
- Nuijs, A. M.; Shuvalov, V. A.; van Gorkom, H. J.; Plijter, J. J.; Duysens, L. N. M. *Biochim. Biophys. Acta* **1986**, *850*, 310.
- Hastings, G.; Kleinherenbrink, F. A. M.; Lin, S.; McHugh, T. J.; Blankenship, R. E. *Biochemistry* **1994**, *33*, 3193.
- Li, Y.-F.; Zhou, W.; Blankenship, R. E.; Allen, J. P. *J. Mol. Biol.* **1997**, *272*, 456.